Available online at www.sciencedirect.com
ScienceDirect
Trans. Nonferrous Met. Soc. China 20(2010) s324−s330
Transactions of Nonferrous Metals Society of China
www.tnmsc.cn

Effects of Ce on microstructure of semi-continuously cast Mg-1.5Zn-0.2Zr magnesium alloy ingots

ZHAO Kai-yang(赵凯阳)[1, 2], PENG Xiao-dong(彭晓东)[1, 2], XIE Wei-dong(谢卫东)[1, 2],
WEI Qun-yi(魏群义)[1, 2], YANG Yan(杨 艳)[1, 2], WEI Guo-bing(魏国兵)[1, 2]

1. College of Materials Science and Engineering, Chongqing University, Chongqing 400045, China;
2. National Engineering Research Center for Magnesium Alloys, Chongqing University, Chongqing, 400044, China

Received 23 September 2009; accepted 30 January 2010

Abstract: Mg-1.5Zn-0.2Zr-*x*Ce (*x*=0, 0.1, 0.3, 0.5, mass fraction, %) alloys were prepared by conventional semi-continuous casting. The effect of rare earth Ce on the microstructure of Mg-1.5Zn-0.2Zr-*x*Ce alloys was studied and the distribution of Ce was analyzed by optical microscopy (OM), X-ray diffractometry (XRD) and scanning electron microscopy (SEM). The results indicate that Ce element exists in the form of $Mg_{12}Ce$ phase and has an obvious refining effect on the microstructure of test alloys. As the Ce content increases, the grain size reduces, the grain boundaries turn thinner, and the distribution of $Mg_{12}Ce$ precipitates becomes more and more dispersed. The Mg-1.5Zn-0.2Zr alloy with 0.3%Ce has the best refinement effect. From center to periphery of the ingot, the amount of granular precipitates in the grain reduces. In longitudinal section of the ingot, some relative long columnar grains appear.
Key words: Mg-1.5Zn-0.2Zr alloy; Ce; semi-continuous casting; refinement

1 Introduction

Magnesium alloy has advantages of low density, high specific strength and damping capacity, and nice electromagnetic shielding, etc[1−2]. As the lightest alloy in structural materials, magnesium alloy is applied more and more extensively in automobile industry, communication, aerospace and others fields. There are die casting magnesium products like motor case, car steering skeleton, mobile phone shell and portable computer shell[3−4], and magnesium extrusion materials with much better performance, like bicycle skeleton, motorcycle shelf, mobile device stent and other products. Besides, magnesium alloy sheet and forging are also applied in 3C electronic products and military products, respectively[5]. However, owing to its hexagonal close-packed (hcp) lattice and few slip system, the plastic deformation capacity of magnesium alloys is poor, which limits the development of wrought magnesium alloys [6−10]. Grain refining is an effective way to improve the deformation structure and properties of magnesium alloys[11]. There are two technical ways to refine dendritic crystals. One is adding modifier to improve the nucleation rate, and the other is accelerating the cooling rate to improve the undercooling of alloy melts.

Rare earth element, which is a good modifier to magnesium alloy, can purify alloys, improve castability and refine microstructure[12]. Nowadays, it is a main way to obtain high quality wrought magnesium alloy billets using the fast cooling way of continuous or semi-continuous casting. In this experiment, the Mg-1.5Zn-0.2Zr alloys with different Ce contents were prepared using conventional semi-continuous casting. Then the effects of Ce contents on the microstructure of semi-continuously cast alloy billets were investigated, the modification mechanism to the microstructure of magnesium alloy was discussed, and the preparation process was optimized.

2 Experimental

The experiment was carried out with the conventional semi-continuous caster. The Mg-1.5Zn-0.2Zr-*x*Ce (*x*=0, 0.1, 0.3, 0.5, mass fraction, %) alloys were prepared by high-purity Mg (99.9%, mass fraction),

Foundation item: Project(2007CB613702) supported by the National Basic Research Program of China; Project(CSTD2006AA4012) supported by the Key Technologies R&D Program of the Chongqing Science and Technology Commission
Corresponding author: PENG Xiao-dong; Tel: +86-23-65111625; Fax: +86-23-65102602; E-mail: pxd@cqu.edu.cn

Zn (99.9%), Mg-25%Ce and Mg-17%Zr master alloys. Firstly, the Mg and Zn billets were put into an electrical resistance furnace and melted under the protection of Ar. When the temperature reached 760 ˚C, the Mg-25%Ce and Mg-17%Zr master alloys were added. After holding for 40 min, the columniform billets with diameter of 80 mm were water cooling cast at 680 ˚C in semi-continuous manner. As shown in Fig.1, the samples are intercepted in the center, 1/2 radius and circle of cross section and longitudinal section of billets. The chemical compositions of the studied alloys and sample numbering are listed in Table 1. The microstructures of the investigated alloys were observed using an optical microscope (OM, OLYMPUS PMG3) and a scanning electron microscope (SEM, JEOL JSM 6460LV) with energy dispersive spectroscopy (EDS) after being polished and corroded by 4% (volume fraction) nitric acid alcohol solution.

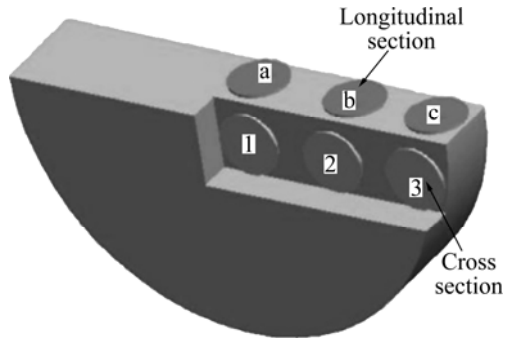

Fig.1 Schematic diagram of sampling parts

3 Results and discussion

3.1 Microstructures of studied alloys before and after adding Ce

Take samples at 1/2 radius of billets for example. Figs.2(a) and (b) show the microstructure of the studied alloys without Ce-addition. As shown in Figs.2(a) and (b), there is uneven microstructure with massive rosaceous grains and wide grain boundaries, and the microstructure consists of dendrites of α-Mg matrix separated by eutectic compounds distributed at the boundaries and some precipitated phase. Under the non-equilibrium solidification conditions, besides small amount of Zn is solid dissolved in Mg, most of Zr is pushed into front of solid-liquid interface, which improves constitutional supercooling to inhibit grain growth, causing the generation of Zn-containing compound phase at the grain boundaries[13]. Besides, owing to solute redistribution during solidification, the grain boundary segregation takes place, and Zn enriches at the boundaries. The SEM images and EDS microanalysis show that there are more Zn in precipitations than at the boundaries and there are more Zn at the boundaries than in the matrix (Fig.3 and Table 2). In the present study, the XRD pattern indicates that no phases are detected except for α-Mg, suggesting that the amount of Zn-containing compound phase is not large enough to be detected (Fig.4). ZHANG[14] found MgZn, $MgZn_2$ and Zn-Zr phases in Mg-Zn-Zr alloy. WU et al[15] identified the phases MgZn, $MgZn_2$ and Mg_4Zn_7 in foundry cast alloy. MOROZOVA et al[16] reported that the as-cast Mg-4.5Zn-0.72Zr alloy contains Mg_2Zn_3, Zn_2Zr_3, ZnZr and Zn_2Zr, by means of physicochemical analysis and XRD. According to the Mg-Zn binary phase diagram, the weak peak in the DSC curve at 410 ˚C corresponds to the melting of Mg_2Zn_3 (Fig.5). Therefore, these eutectic compounds and precipitations in the studied alloys can be proved as Mg_2Zn_3 phase.

It can also be seen from Fig.2 that Ce has an obvious refinement effect on the studied alloys, and some granular precipitates appear in the microstructure. Due to the addition of 0.1% Ce, the massive rosaceous grains in the microstructure are crushed into fine equiaxed grains, the amount of granular phase increases significantly, and the grain boundaries become thinner. As the Ce content increases, the grain size reduces gradually, and the amount of precipitates in the microstructure (especially in the boundaries) becomes larger and larger. When the Ce content reaches 0.3%, the grain size is the smallest, the amount of precipitates in the microstructure is the largest and the distribution of the precipitates is the most dispersed. The XRD patterns show that the new phase $Mg_{12}Ce$ appears when Ce is added into Mg-1.5Zn-0.2Zr alloy (Fig.4). This new phase has an effect of dispersion strengthening. It can inhibit the grain boundary sliding, improve the thermal stability of the studied alloys, and then optimize the mechanical properties of the studied alloys. When the Ce content is 0.5%, the grain size does not turn smaller, but the grain-

Table 1 Chemical compositions of investigated alloys (mass fraction, %) and samples number

w(Zn)/%	*w*(Zr)/%	*w*(Ce)/%	*w*(Mg)/%	Sample No.						
				Alloy	Cross section			Longitudinal section		
					Position 1	Position 2	Position 3	Position a	Position b	Position c
1.5	0.2	−	Bal.	1#	1-1#	1-2#	1-3#	1-a#	1-b#	1-c#
1.5	0.2	0.1	Bal.	2#	2-1#	2-2#	2-3#	2-a#	2-b#	2-c#
1.5	0.2	0.3	Bal.	3#	3-1#	3-2#	3-3#	3-a#	3-b#	3-c#
1.5	0.2	0.5	Bal.	4#	4-1#	4-2#	4-3#	4-a#	4-b#	4-c#

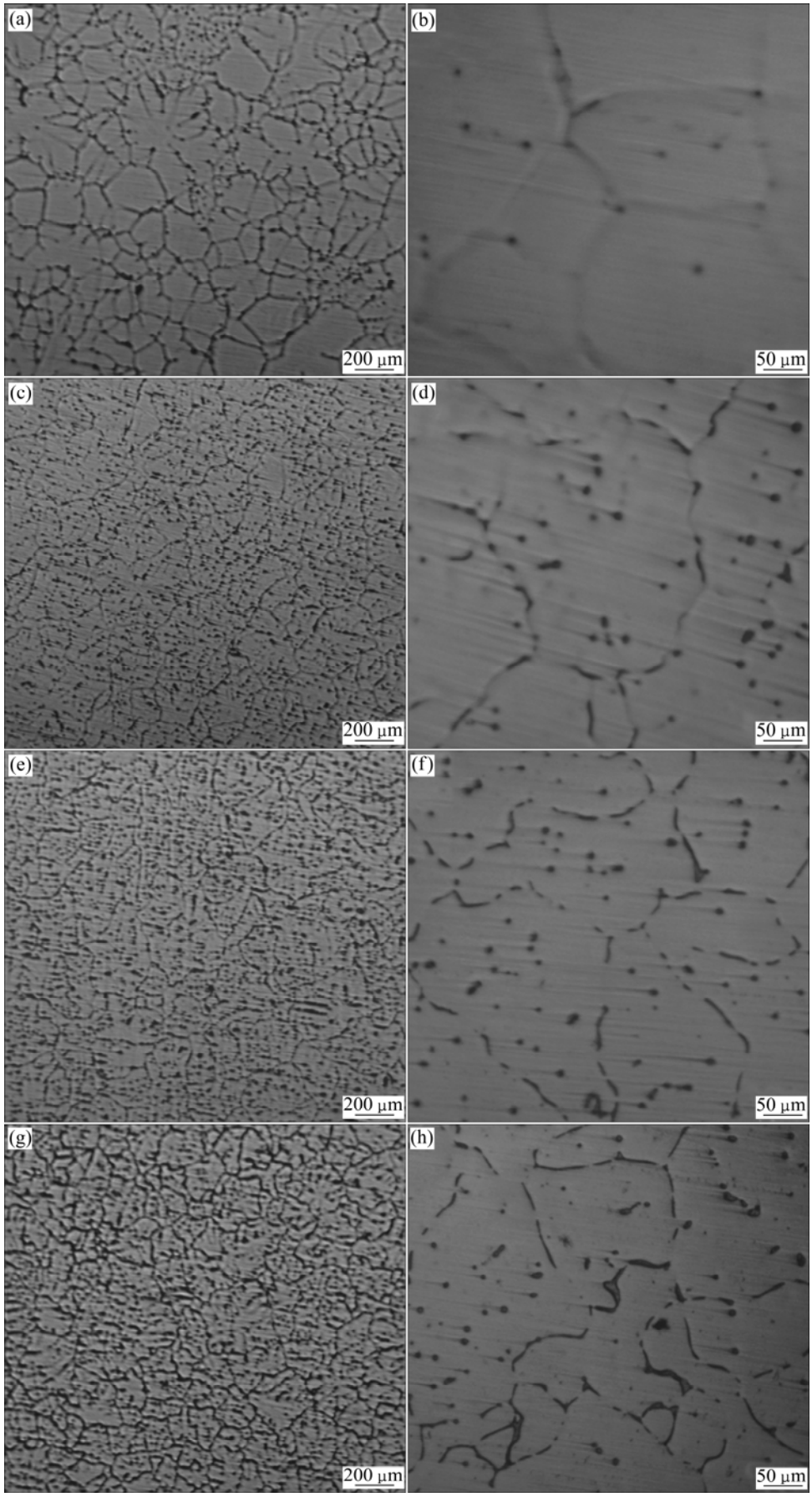

Fig.2 Optical micrographs of 1/2 radius of four ingots: (a), (b) Sample 1-2#; (c), (d) Sample 2-2#; (e), (f) Sample 3-2#; (g), (h) Sample 4-2#

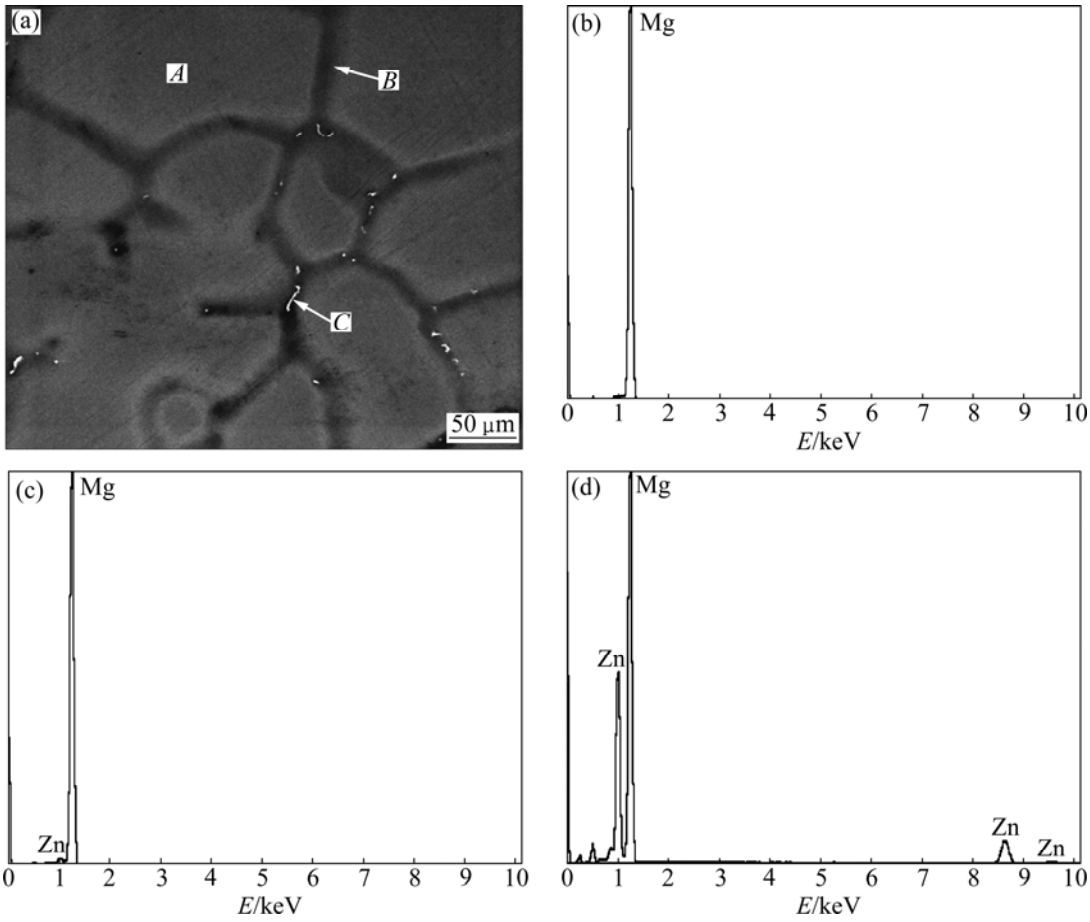

Fig.3 SEM image of sample 1-2# and EDS spectra in positions *A*, *B* and *C*: (a) SEM image of sample 1-2#; (b) EDS spectrum in position *A*; (c) EDS spectrum in position *B*; (d) EDS spectrum in position *C*

Table 2 EDS analysis results in positions *A*, *B* and *C* (in Fig.3(a))

Position	Mg		Zn	
	w/%	*x*/%	*w*/%	*x*/%
A	100.00	100.00	0	0
B	98.09	99.28	1.91	0.72
C	65.36	83.53	34.64	16.47

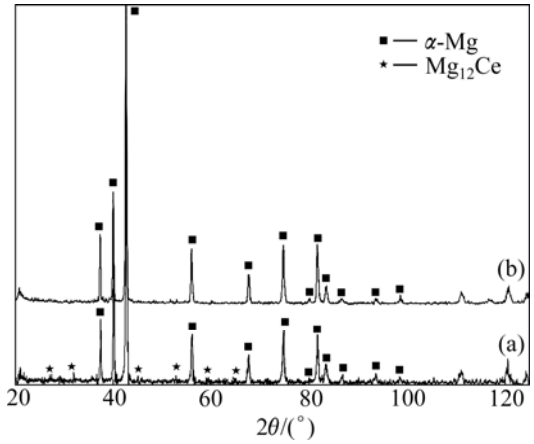

Fig.4 XRD patterns of Mg-1.5Zn-0.2Zr-0.5Ce alloy (a) and Mg-1.5Zn-0.2Zr alloy (b)

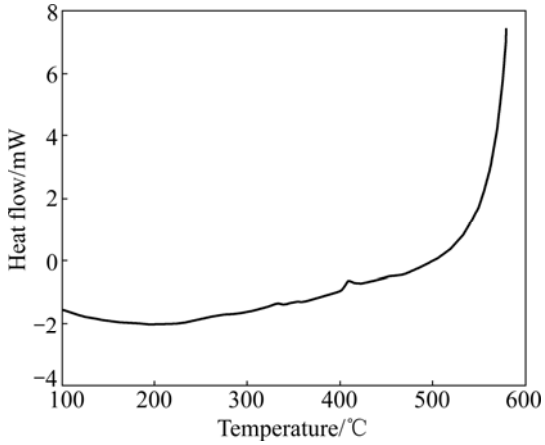

Fig.5 DSC curve of Mg-1.5Zn-0.2Zr alloy

boundary segregation becomes thicker with the morphology of nearly continuous network, and there are nonuniform precipitates. In a word, 0.3% is the best amount of Ce content to the studied alloy.

3.2 Microstructures of three different areas of billet

Taking sample 4# for example, the microstructure composes of all equiaxed grains. During solidification process, the cooling rates of three areas of the billet are

significantly different, and the composition segregation exists, which causes obviously different microstructures. There are many granular precipitates dispersively distributed in the center and 1/2 radius of the ingot, but fewer in the circle area. As Ce equilibrium partition coefficient $k<1$, Ce enriches along the solid-liquid interface and precipitated dispersedly in the form of granular $Mg_{12}Ce$ phase during solidification process. Due to the large size of billets, the cooling rate decreases gradually from circle to center area. So, Ce has enough time to segregate from the matrix, causing that the amount of intragranular precipitates of Ce-containing phase particles becomes more and more.

As shown in Fig.6, the grains in the cross section are equiaxed; while in longitudinal section of the billets, as shown in Fig.7, there are some long columnar grains in sample 3# and rosaceous grains in sample 4#.

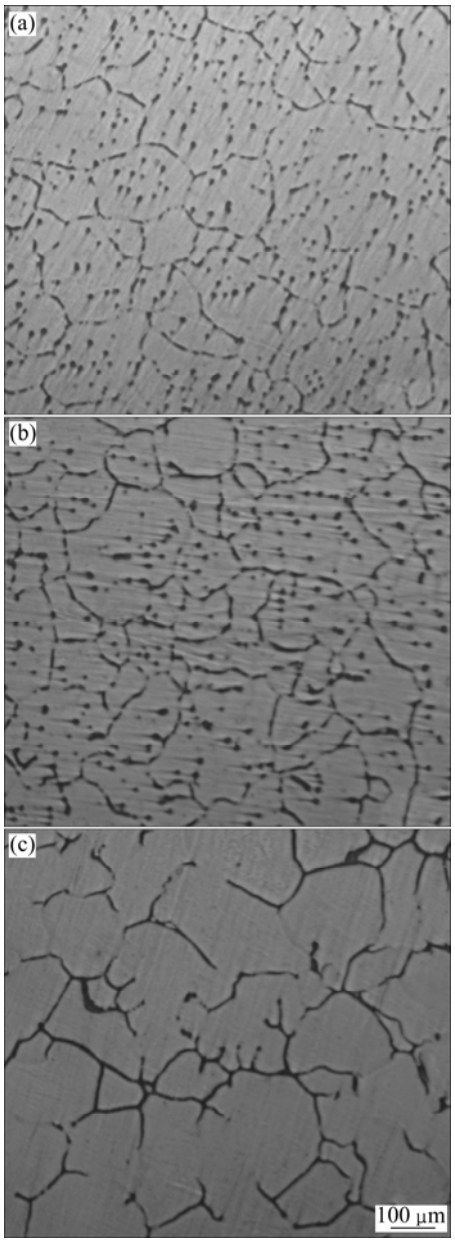

Fig.6 Optical micrographs of three areas of Mg-1.5Zn-0.2Zr-0.5Ce alloy ingot: (a) Sample 4-1#; (b) Sample 4-2#; (c) Sample 4-3#

4 Discussion

4.1 Effects of Ce on microstructure

Owing to a solid solubility limit of only 0.5%, Ce atoms are mainly pushed into front of solid-liquid interface during solidification, effectively inhibiting grain growth. The degree of constitutional supercooling to promote nucleation is improved. Also, the dendrites divorce into narrow necking down, which is prone to fuse and shed. Hence the grains are refined.

Moreover, Ce is a surface active element to Mg, and it has a positive absorption effect. In this experiment, Ce moves to the surface of dendrites during solidification, making the concentration higher at the surface than grain inner. Then the surface tension of Mg alloy melt decreases consequently, lowering the nucleation energy of critical nucleus, and the nucleation rate increases. The activity of Ce can be expressed by Gibbs adsorption equation as follows:

$$G=-\frac{C}{RT}\cdot\frac{\mathrm{d}\sigma}{\mathrm{d}c} \tag{1}$$

where G is the amount of solute absorpted positively or negatively from per unit area of liquid surface, σ is the surface tension, c is the solute concentration, T is the absolute temperature, and R is the gas constant[17].

It can be seen from Eq.(1) that, if $G>0$, $\mathrm{d}\sigma/\mathrm{d}c<0$, which means that with the addition of Ce, the surface tension of Mg alloy melt decreases. So it is proved that Ce is a surface active element to Mg alloy.

Due to the addition of Ce with high melting point, more condensation nucleus are generated during solidification from liquid to solid in the studied alloys, and therefore, the microstructure is refined, and the surface area becomes larger. Then the grain boundaries turn to thinner as the volume of boundary phase stays invariable. In addition, a large amount of $Mg_{12}Ce$ new phase appears after adding Ce into the studied alloys, which reduces the probability of the generation and growth of Mg_2Zn_3 phase. Hence it can be seen from the comparison of metallographs (Fig.2) that the grain boundaries become thinner, and the distribution becomes much more dispersed with Ce addition.

4.2 Effects of constitutional supercooling on microstructure

Due to the solute redistribution during solidification process, the solute in front of solid-liquid interface is segregated and the constitutional supercooling appears. The constitutional supercooling criterion is as follows:

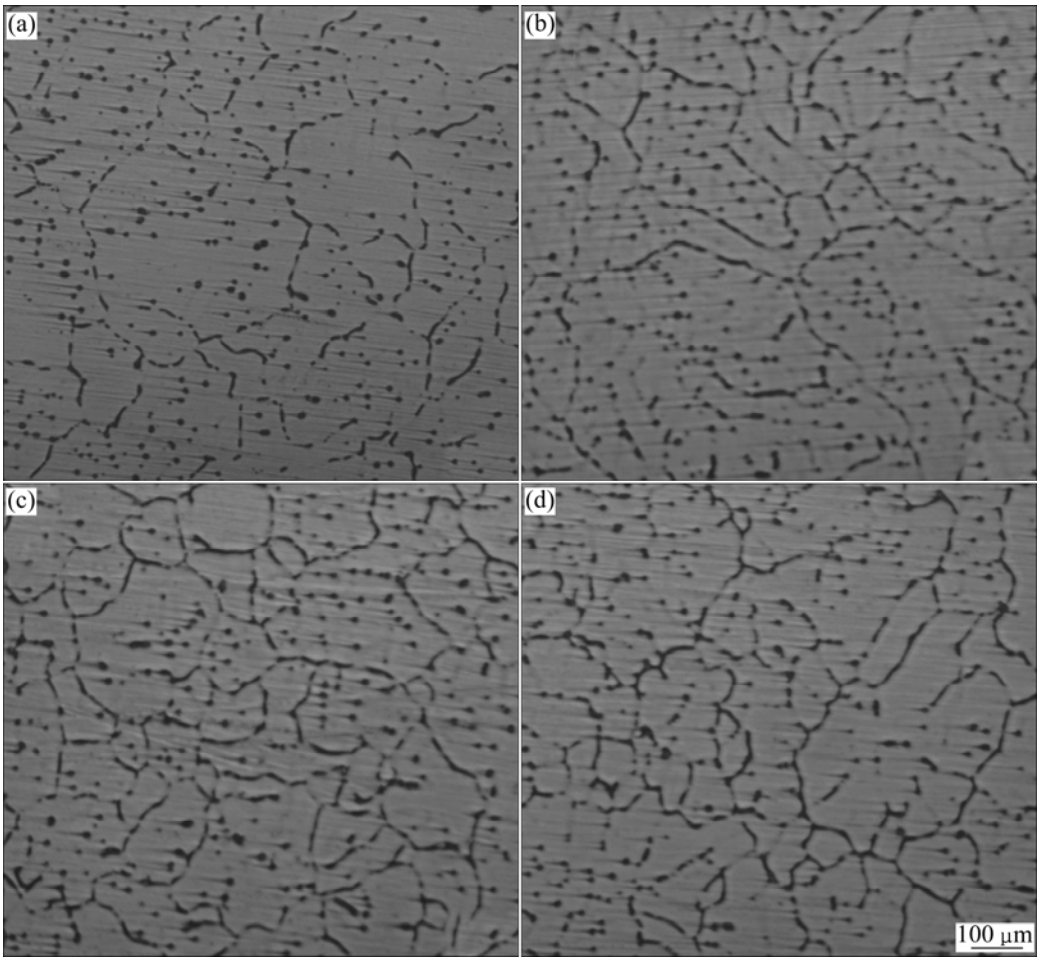

Fig.7 Optical micrographs of 1/2 radius of cross section and longitudinal section of Mg-1.5Zn-0.2Zr-0.3Ce and Mg-1.5Zn-0.2Zr-0.5Ce alloys: (a) Sample 3-2#; (b) Sample 3-b#; (c) Sample 4-2#; (d) Sample 4-b#

$$\frac{G_L}{\nu} < \frac{m_L c_0 (1-k)}{D_L k} \tag{2}$$

where G_L is the temperature gradient in front of solid-liquid interface, c_0 is the original composition, k is the solute equilibrium partition coefficient, D_L is the diffusion coefficient of solute in liquid phase, ν is the cooling rate, and m_L is a constant[17]. $m_L c_0(1-k)/(D_L k)$ can be substituted by ΔT, which is the crystallization range of alloys with the original composition of c_0.

This criterion shows that, the larger the G_L, the smaller the ν, the larger the G_L/ν, and the less the beneficial to constitutional supercooling. Contrarily, the smaller the G_L, the larger the ν, the smaller the G_L/ν, and the more the beneficial to constitutional supercooling causing solute segregation. And the larger the crystallization range of alloys, the larger the trend of constitutional supercooling, and the larger the segregation degree of solute.

As seen from Mg-Ce phase diagram, when the Ce content is less than 0.52%, the crystallization range of the studied alloys increases gradually with Ce content. So, when the Ce content is 0.5%, the segregation degree of solute is the largest, and the amount of particle phase is the biggest. But the alloy with 0.5% Ce has less uniform boundaries than the alloy with 0.3% Ce. So 0.3% is the best amount of Ce content to the studied alloy.

4.3 Effects of secondary cooling on microstructure

The cooling intensity of continuously casting ingot mainly depends on cooling water volume or pressure. The heat of billets is conducted out 15%−20% of all in crystallizer first cooling, and the other heat is conducted out through secondary cooling[18]. Effects of secondary cooling is to assure that the heat is conducted along axial direction (billet drawing direction), promoting axial solidification, lowing the depth of liquid cave, and then to obtain the compact microstructure. As those grains grow in priority during solidification process of casting, the morphology turns to columnar due to unidirectional heat conduction. Some rosaceous and columnar grains appear in the longitudinal section of billets, because of the unidirectional heat conduction caused by secondary cooling.

5 Conclusions

1) The rare earth element Ce can refine the microstructure of Mg-1.5Zn-0.2Zr alloys in the semi-continuously casting process.

2) The amount of precipitates increases with Ce content, and decreases from center to circle area of billets. When the Ce content is 0.3%, the distribution of precipitates is the most dispersed.

3) Under the influence of unidirectional heat conduction factor caused by secondary cooling, there are coarse rosaceous and columnar grains in the longitudinal section of billets.

References

[1] ZHOU Hong, LI Wei, WANG Ming-xing, ZHAO Yu. Study on ignition proof AZ91D magnesium alloy chips with cerium addition [J]. Journal of Rare Earths, 2005, 23(4): 466−469.

[2] ELIEZER A, GUTMAN E M. Corrosion fatigue of die-cast and extruded magnesium alloys [J]. Journal of Light Materials, 2001, 1(3): 179−186.

[3] POLMEAR I J. Magnesium alloys and applications [J]. Materials Science and Technology, 1994, 10(1): 1−16.

[4] MORDIKE B L, EBERT T. Magnesium: properties—applications—potential [J]. Mater Sci Eng A, 2001, 302: 37−45.

[5] ZHANG Ding-fei, LAN Wei, ZENG Ding-ding, ZHANG Bao-ping. Quantitative relationship between secondary dendrite arm spacing and solidification cooling rate of AZ31 magnesium alloy [J]. Heat Treatment of Metals, 2008, 33(3): 1−3. (in Chinese)

[6] FANG Xi-ya, YI Dan-qing, LUO Wen-hai, WANG Bin, ZHANG Xiao-juan, ZHENG Feng. Effects of yttrium on recrystallization and grain growth of Mg-4.9Zn-0.7Zr alloy [J]. Journal of Rare Earths, 2008, 26(3): 392−397.

[7] POLMEAR I J. Recent developments in light alloys [J]. Trans JIM, l996, 37(1): 12−31.

[8] IDRIS M H. Precision casting of a magnesium-base alloy [J]. Foundryman, 1997, 90(4): 140−144.

[9] IDRIS M H. Processing and evaluation of investment cast magnesium-base alloy [J]. AFS Trans, 1996, 104(20/23): 237−244.

[10] DOEGE E, DRODER K. Sheet metal forming of magnesium wrought alloys-formability and process technology [J]. Journal of Materials Processing Technology, 2001, 115(1): 14−19.

[11] CHEN Gang, FAN Pei-geng, PENG Xiao-dong, CAO Peng-jun, CAI Wei. Efect of Sr addition on the microstructure and the properties of AZ91 magnesium alloy [J]. Light Alloy Fabrication Technology, 2008, 36(8): 15−18. (in Chinese)

[12] ZHANG Jing-huai, TANG Ding-xiang, ZHANG Hong-jie, WANG Li-min, WANG Jun, MENG Jia. Efect and application of rare earth element in magnesium alloys [J]. Rare Metals, 2008, 32(5): 659−667. (in Chinese)

[13] LUO Wen-hai, YI Dan-qing, WANG Bin, FANG Xi-ya, GU Wei, ZHOU Ling-ling. Microstructure and mechanical properties of Mg-4.9Zn-0.9Y-0.7Zr alloy [J]. Journal of Materials Science & Engineering, 2006, 24(6): 241−243. (in Chinese)

[14] ZHANG Shao-qing. Strengthening effects of rare earths on wrought Mg-Zn-Zr-RE alloys [C]// The Symposium of the 3rd Annual Meeting of Physical and Chemical Test Institution. Beijing: Chinese Mechanical Engineering Society, 1984: 270−274. (in Chinese)

[15] WU An-ru, XIA Chang-qing, DONG Li-jun. Distributing, evolvement and effect on the mechanical properties of the rare-earth Ce, Y in ZK60 alloys [J]. Rare Metal Materials and Engineering, 2007, 36(11): 1955−1959. (in Chinese)

[16] MOROZOVA G I, TIKHONOVA V V, LASHKO N F. Phase composition and mechanical properties of cast Mg-Zn-Zr alloys [J]. Met Sci Heat Treat: Engl Trans, 1978, 20: 650−657.

[17] WANG Shou-peng. Theoretical and process fundamental of castings [M]. Xi'an: Northwestern Polytechnical University Press, 1994: 14−126. (in Chinese)

[18] ZHANG Si-qi, HUANG Jin-song. Melting and ingots of nonferrous metals [M]. Beijing: Chemical Industry Press, 2006: 113. (in Chinese)

(Edited by HE Xue-feng)